Nucleon electromagnetic form factors and axial charge from $N_f = 2 + 1$ CLS ensembles

Stefano Capitani, Dalibor Djukanovic, Tim Harris*, Georg von Hippel,
Parikshit Junnarkar, Harvey Meyer, Hartmut Wittig

HELMHOLTZ ASSOCIATION
Helmholtz Institute Mainz

JOHANNES GUTENBERG UNIVERSITÄT MAINZ

JG|U

Lattice 2015 (Kobe), July 18

Outline

Lattice set-up and simulation details

Systematics due to excited states

Preliminary results on G_E and G_M

Preliminary results on g_A

Motivation

We wish to access nucleon form factors, $G_{A,P}$ and $F_{1,2}$ from the matrix elements

$$\langle N(\boldsymbol{p'},s')|\,\bar{\psi}\gamma_\mu\psi\,|N(\boldsymbol{p},s)\rangle = \bar{u}(\boldsymbol{p'},s')\left[\gamma_\mu F_1(Q^2) + i\frac{\sigma_{\mu\nu}q_\nu}{2m_N}F_2(Q^2)\right]u(\boldsymbol{p},s),$$

$$\langle N(\boldsymbol{p'},s')|\,\bar{\psi}\gamma_5\gamma_\mu\psi\,|N(\boldsymbol{p},s)\rangle = \bar{u}(\boldsymbol{p'},s')\left[\gamma_5\gamma_\mu G_A(Q^2) + \frac{\gamma_5 q_\mu}{2m_N}G_P(Q^2)\right]u(\boldsymbol{p},s)$$

with, in future, control over systematic uncertainties due to cut-off, non-physical pion mass and excited states, to confront with experiment.

Here, we examine the Sachs electromagnetic form factors

$$G_E(Q^2) = F_1(Q^2) - \frac{Q^2}{2m_N^2}F_2(Q^2),$$

$$G_M(Q^2) = F_1(Q^2) + F_2(Q^2)$$

and the benchmark axial charge, $g_A = G_A(0)$, on CLS $N_f = 2+1$ open bcs ensembles.

Motivation

We wish to access nucleon form factors, $G_{A,P}$ and $F_{1,2}$ from the matrix elements

$$\langle N(\boldsymbol{p'}, s')|\,\bar{\psi}\gamma_\mu\psi\,|N(\boldsymbol{p}, s)\rangle = \bar{u}(\boldsymbol{p'}, s')\left[\gamma_\mu F_1(Q^2) + i\frac{\sigma_{\mu\nu}q_\nu}{2m_N}F_2(Q^2)\right]u(\boldsymbol{p}, s),$$
$$\langle N(\boldsymbol{p'}, s')|\,\bar{\psi}\gamma_5\gamma_\mu\psi\,|N(\boldsymbol{p}, s)\rangle = \bar{u}(\boldsymbol{p'}, s')\left[\gamma_5\gamma_\mu G_A(Q^2) + \frac{\gamma_5 q_\mu}{2m_N}G_P(Q^2)\right]u(\boldsymbol{p}, s)$$

with, in future, control over systematic uncertainties due to cut-off, non-physical pion mass and excited states, to confront with experiment.

Here, we examine the Sachs electromagnetic form factors

$$G_E(Q^2) = F_1(Q^2) - \frac{Q^2}{2m_N^2}F_2(Q^2),$$
$$G_M(Q^2) = F_1(Q^2) + F_2(Q^2)$$

and the benchmark axial charge, $g_A = G_A(0)$, on CLS $N_f = 2+1$ open bcs ensembles.

CLS effort

name	β	a (fm)	T/a	L/a	$m_\pi L$	m_π (MeV)	N_{meas}
H102	3.4	0.086	96	32	5.8	350	7988
H105	"	"	"	"	4.9	280	7348
C101	"	"	"	48	4.7	220	4256
~~N200~~	~~3.55~~	~~0.06~~	~~128~~	~~48~~	~~4.4~~	~~280~~	~~3200~~

CLS open bcs $N_{\mathrm{f}} = 2 + 1$ ensembles used in this work

$N_{\mathrm{f}} = 2 + 1$ flavours of $O(a)$-improved Wilson clover fermion.

[Bruno et al.]

Open boundary conditions in time combat poor scaling of autocorrelation of topological charge as $a \to 0$.

[Lüscher, Schäfer]

Twisted-mass regulator guards against exceptional configurations.

[Lüscher, Palombi]

We use SAP+GCR solver from openQCD for measurements.

Ratio method

$J(\boldsymbol{y}, t)e^{i\boldsymbol{q}\boldsymbol{y}}$

$$C_{3,J}(t, t_s; \boldsymbol{q}) = \Gamma \langle \sum_{\boldsymbol{x},\boldsymbol{y}} N(\boldsymbol{x}, t_s) e^{i\boldsymbol{p}\boldsymbol{x}}$$

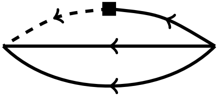

$$\bar{N}(0) \rangle$$

$$R_J(t, t_s; Q^2) = \frac{C_{3,J}(t, t_s; \boldsymbol{q})}{C_2(t_s; \boldsymbol{q})} \sqrt{\frac{C_2(t_s - t; -\boldsymbol{q}) C_2(t, \boldsymbol{0}) C_2(t_s; \boldsymbol{0})}{C_2(t_s - t; \boldsymbol{0}) C_2(t; -\boldsymbol{q}) C_2(t_s; -\boldsymbol{q})}}$$

[Alexandrou et al.]

Lattice estimates for form factors contain excited states,.... Denote effective ones e.g. for isovector vector and axial vector

$$G_E^{\text{eff}}(Q^2) = \sqrt{\frac{2E_{Q^2}}{m + E_{Q^2}}} R_{V_0}(t, t_s; Q^2), \qquad g_A^{\text{eff}} = -iR_{A_3}(t, t_s; Q^2 = 0).$$

Ratio method

$$C_{3,J}(t,t_s;\boldsymbol{q}) = \Gamma\left\langle \sum\nolimits_{\boldsymbol{x},\boldsymbol{y}} N(\boldsymbol{x},t_s)e^{i\boldsymbol{p}\boldsymbol{x}}\right.$$

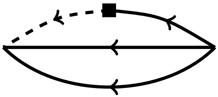

$$\left.\bar{N}(0)\right\rangle$$

$$R_J(t,t_s;Q^2) = \frac{C_{3,J}(t,t_s;\boldsymbol{q})}{C_2(t_s;\boldsymbol{q})}\sqrt{\frac{C_2(t_s-t;-\boldsymbol{q})C_2(t,\boldsymbol{0})C_2(t_s;\boldsymbol{0})}{C_2(t_s-t;\boldsymbol{0})C_2(t;-\boldsymbol{q})C_2(t_s;-\boldsymbol{q})}}$$

[Alexandrou et al.]

Lattice estimates for form factors contain excited states,.... Denote effective ones e.g. for isovector vector and axial vector

$$G_E^{\text{eff}}(Q^2) = \sqrt{\frac{2E_{Q^2}}{m+E_{Q^2}}}R_{V_0}(t,t_s;Q^2), \qquad g_A^{\text{eff}} = -iR_{A_3}(t,t_s;Q^2=0).$$

Measurement set-up

Boundaries contribute excitations with vacuum quantum numbers, e.g.

$$C_2(t, \mathbf{0}) = \ldots + \langle 2\pi | \, N \, | N \rangle \, \langle N | \, \bar{N} \, | 0 \rangle \, e^{-2m_\pi (T-t)}$$

when one operator close to the boundary at $t = T$.

Effects on baryon two-point function investigated: no boundary effects unless much closer than $\lesssim T/4a$.

Fix source in bulk, displace only in spatial volume, e.g. for $T/a = 96$, $T/L = 3$,

$$(t_{\rm src}/a, \boldsymbol{x}_{\rm src}/a) \in \{(40, 0, 0, 0), (40, 16, 16, 0), (40, 16, 0, 16), (40, 0, 16, 16)\}$$

for three source-sink separations $1\text{fm} \lesssim t_s = 12a, 14a, 16a \lesssim 1.4\text{fm}$.

Gaussian smeared sources with APE smeared links

Smearing parameters $(N_{\rm steps}, \alpha) = (75, 1.1)$ optimized from nucleon effective mass.

Smearing radius saturates after $\alpha \approx 0.6$.

Measurement set-up

Boundaries contribute excitations with vacuum quantum numbers, e.g.

$$C_2(t,\mathbf{0}) = \ldots + \langle 2\pi|\, N\,|N\rangle\,\langle N|\,\bar{N}\,|0\rangle\, e^{-2m_\pi(T-t)}$$

when one operator close to the boundary at $t = T$.

Effects on baryon two-point function investigated: no boundary effects unless much closer than $\lesssim T/4a$.

Fix source in bulk, displace only in spatial volume, e.g. for $T/a = 96$, $T/L = 3$,

$$(t_{\mathrm{src}}/a, \boldsymbol{x}_{\mathrm{src}}/a) \in \{(40,0,0,0),(40,16,16,0),(40,16,0,16),(40,0,16,16)\}$$

for three source-sink separations $1\mathrm{fm} \lesssim t_s = 12a, 14a, 16a \lesssim 1.4\mathrm{fm}$.

Gaussian smeared sources with APE smeared links

Smearing parameters $(N_{\mathrm{steps}}, \alpha) = (75, 1.1)$ optimized from nucleon effective mass.

Smearing radius saturates after $\alpha \approx 0.6$.

Measurement set-up

Boundaries contribute excitations with vacuum quantum numbers, e.g.

$$C_2(t,\mathbf{0}) = \ldots + \langle 2\pi|\, N\,|N\rangle\,\langle N|\,\bar{N}\,|0\rangle\, e^{-2m_\pi(T-t)}$$

when one operator close to the boundary at $t = T$.

Effects on baryon two-point function investigated: no boundary effects unless much closer than $\lesssim T/4a$.

Fix source in bulk, displace only in spatial volume, e.g. for $T/a = 96$, $T/L = 3$,

$$(t_{\mathrm{src}}/a, \boldsymbol{x}_{\mathrm{src}}/a) \in \{(40,0,0,0),(40,16,16,0),(40,16,0,16),(40,0,16,16)\}$$

for three source-sink separations $1\mathrm{fm} \lesssim t_s = 12a, 14a, 16a \lesssim 1.4\mathrm{fm}$.

Renormalization

For $J(x) = V_\mu(x)$ use point-split discretization.

For axial charge $J(x) = A_3(x)$, use preliminary ALPHA Z_A.

[Bulava, Della Morte; Lattice 2014]

Reweighting

Reminder

$$\langle O\rangle = \frac{\langle Ow\rangle_w}{\langle w\rangle_w}, \quad \text{where} \quad \langle O\rangle_w = \frac{\int \mathrm{d}U w^{-1} O e^{-S}}{\int \mathrm{d}U w^{-1} e^{-S}}$$

$$var_w(O) = \langle w^{-1}\rangle\langle (O-\bar{O})^2 w\rangle$$

Reweighting factors estimated stochastically.

In this work, we use chains with same physics parameters but different simulation parameters (Hasenbusch masses,. . .).

Take weighted average from different chains.

Impact of reweighting on gluonic and mesonic observables has been investigated.
[Bruno et al.; Lattice 2014]

Nucleon effective mass

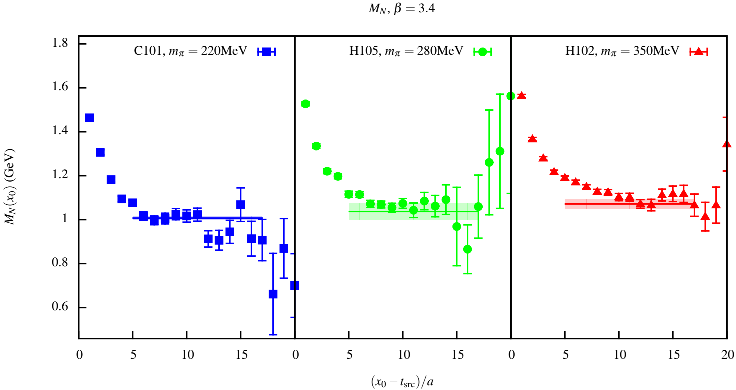

Multi-exponential fits to the correlator

Excited-state systematics

With increased precision, previous experience suggests importance of accounting for excited states with gaps to next highest states Δ and Δ',

$$G_X^{\mathrm{eff}}(t, t_s, Q^2) = G_X(Q^2) + O(e^{-\Delta t}) + O(e^{-\Delta'(t_s - t)})$$

Summed operator insertions method

$$S_X(t_s; Q^2)/a \equiv \sum_{t=a}^{t_s-a} G_X^{\mathrm{eff}}(t, t_s; Q^2) = c_X(Q^2) + t_s \hat{G}_X(Q^2)$$

$\hat{G}_X$ has $O(e^{-\Delta t_s})$ corrections

Two-state fit

$$G_X^{\mathrm{eff}}(t, t_s, Q^2) = \hat{G}_X(Q^2) + c_{1,X}(Q^2)e^{-\Delta t} + c_{2,X}(Q^2)e^{-\Delta'(t_s - t)}$$

Evidence that interacting finite-volume $N\pi$ levels very close to non-interacting case.
[Hansen et al.; to appear]

Fix gap to m_π or $2m_\pi$ where appropriate.

Excited-state systematics

With increased precision, previous experience suggests importance of accounting for excited states with gaps to next highest states Δ and Δ',

$$G_X^{\text{eff}}(t, t_s, Q^2) = G_X(Q^2) + O(e^{-\Delta t}) + O(e^{-\Delta'(t_s - t)})$$

Summed operator insertions method

$$S_X(t_s; Q^2)/a \equiv \sum_{t=a}^{t_s - a} G_X^{\text{eff}}(t, t_s; Q^2) = c_X(Q^2) + t_s \hat{G}_X(Q^2)$$

$\hat{G}_X$ has $O(e^{-\Delta t_s})$ corrections

Two-state fit

$$G_X^{\text{eff}}(t, t_s, Q^2) = \hat{G}_X(Q^2) + c_{1,X}(Q^2) e^{-\Delta t} + c_{2,X}(Q^2) e^{-\Delta'(t_s - t)}$$

Evidence that interacting finite-volume $N\pi$ levels very close to non-interacting case.
[Hansen et al.; to appear]

Fix gap to m_π or $2m_\pi$ where appropriate.

Excited-state systematics

With increased precision, previous experience suggests importance of accounting for excited states with gaps to next highest states Δ and Δ',

$$G_X^{\text{eff}}(t, t_s, Q^2) = G_X(Q^2) + O(e^{-\Delta t}) + O(e^{-\Delta'(t_s - t)})$$

Summed operator insertions method

$$S_X(t_s; Q^2)/a \equiv \sum_{t=a}^{t_s - a} G_X^{\text{eff}}(t, t_s; Q^2) = c_X(Q^2) + t_s \hat{G}_X(Q^2)$$

$\hat{G}_X$ has $O(e^{-\Delta t_s})$ corrections

Two-state fit

$$G_X^{\text{eff}}(t, t_s, Q^2) = \hat{G}_X(Q^2) + c_{1,X}(Q^2) e^{-\Delta t} + c_{2,X}(Q^2) e^{-\Delta'(t_s - t)}$$

Evidence that interacting finite-volume $N\pi$ levels very close to non-interacting case.
[Hansen et al.; to appear]

Fix gap to m_π or $2m_\pi$ where appropriate.

Preliminary G_E at fixed $Q^2 = 0.20\text{GeV}^2$, $m_\pi = 350\text{MeV}$

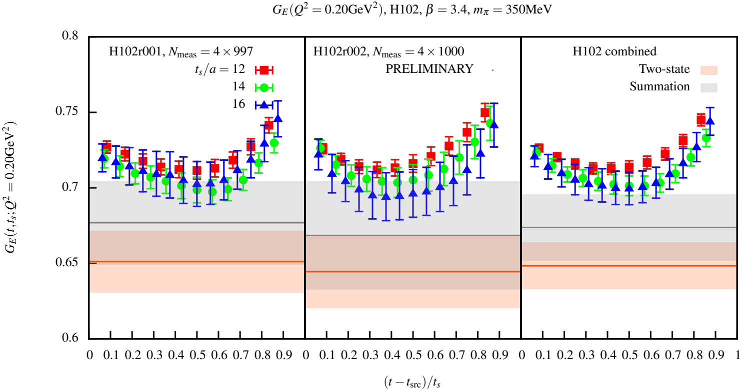

- $(t_s) = (12a, 14a, 16a) = (1.03\text{fm}, 1.20\text{fm}, 1.38\text{fm})$

Preliminary G_M at fixed $Q^2 = 0.81\text{GeV}^2$, $m_\pi = 350\text{MeV}$

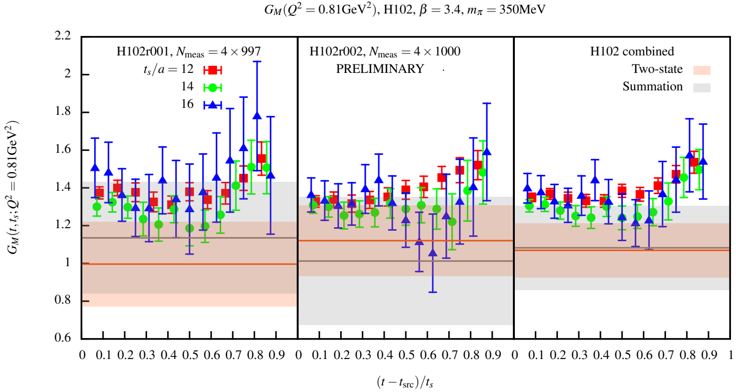

▷ $(t_s) = (12a, 14a, 16a) = (1.03\text{fm}, 1.20\text{fm}, 1.38\text{fm})$

Preliminary G_E, G_M versus Q^2, $m_\pi = 350\text{MeV}$

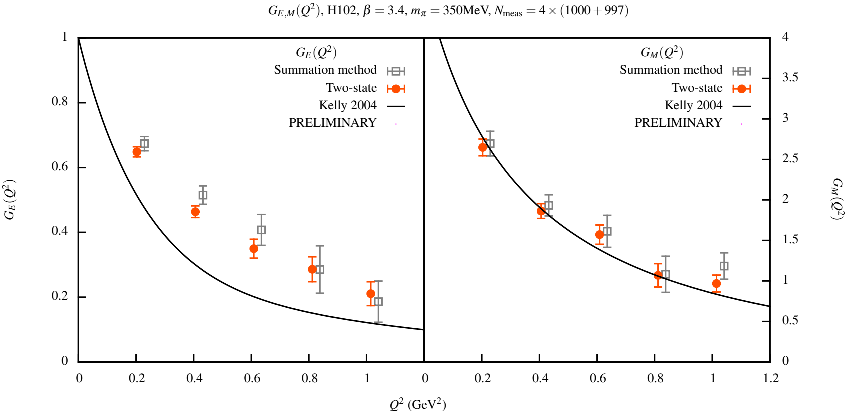

Preliminary G_E, G_M versus Q^2, $m_\pi = 280\text{MeV}$

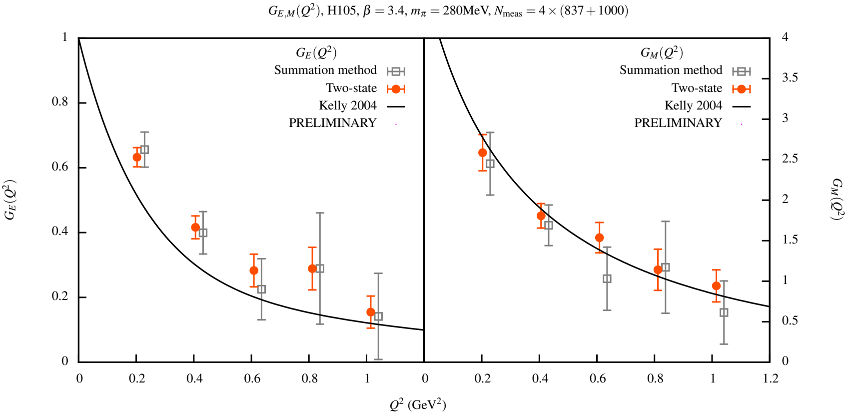

Preliminary G_E, G_M versus Q^2, $m_\pi = 220\text{MeV}$

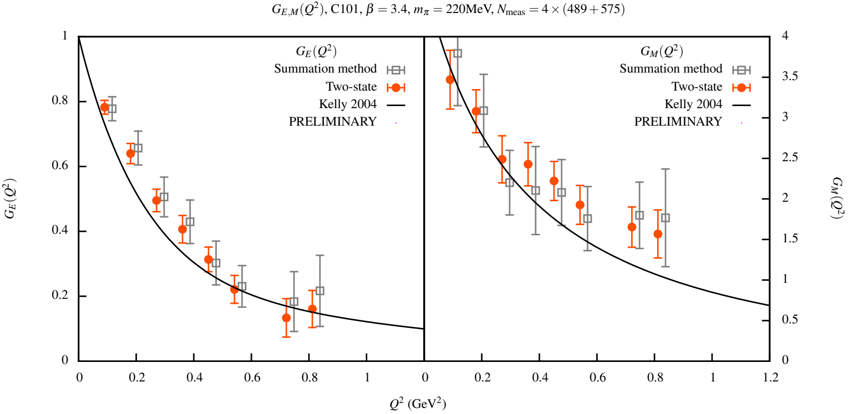

Preliminary G_E, G_M versus Q^2

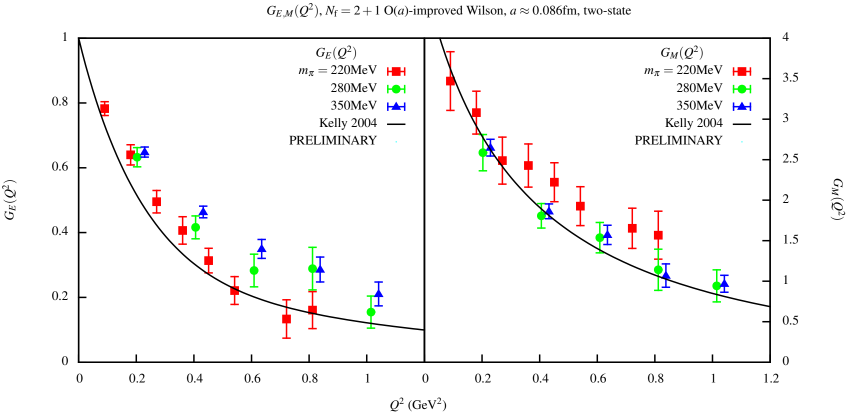

Comparison with $N_f = 2$ Wilson clover

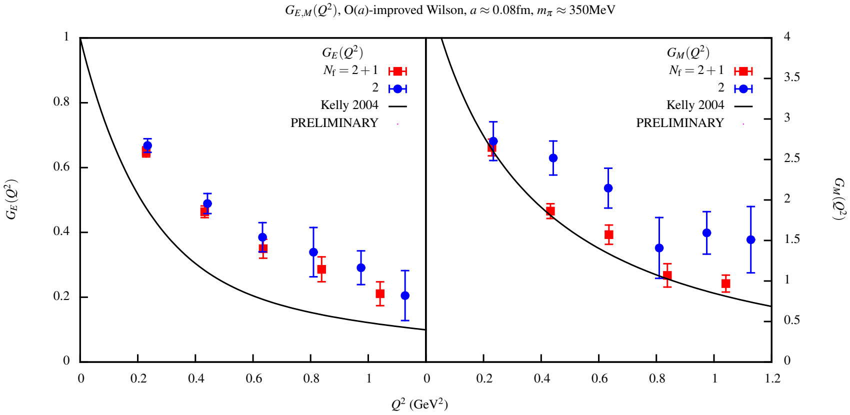

Warning: different chiral trajectory for $N_f = 2$ and $N_f = 2 + 1$

Preliminary g_A, $m_\pi = 280\text{MeV}$

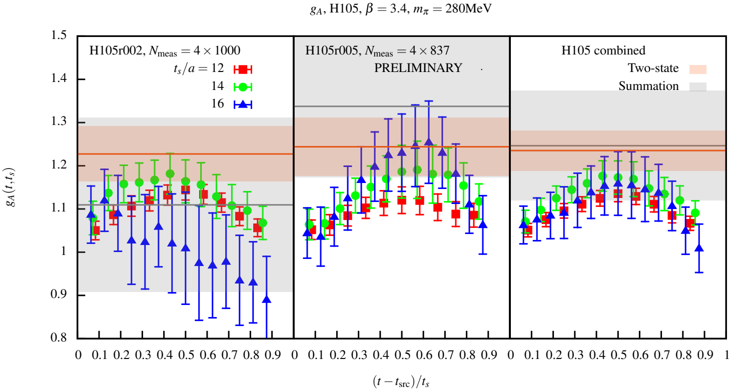

- $(t_s) = (12a, 14a, 16a) = (1.03\text{fm}, 1.20\text{fm}, 1.38\text{fm})$

Preliminary g_A, $m_\pi = 220\mathrm{MeV}$

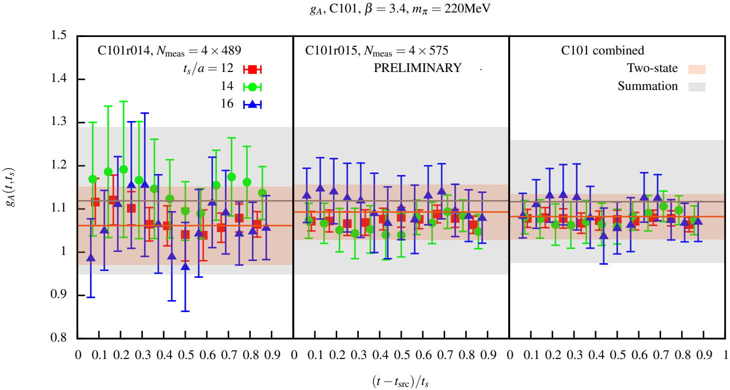

- $(t_s) = (12a, 14a, 16a) = (1.03\mathrm{fm}, 1.20\mathrm{fm}, 1.38\mathrm{fm})$

Preliminary g_A

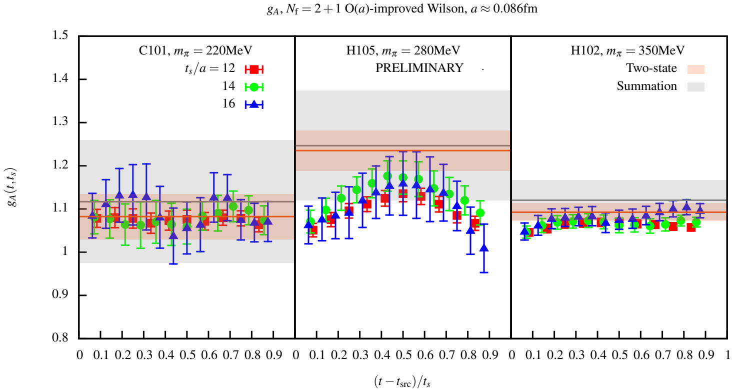

▷ $(t_s) = (12a, 14a, 16a) = (1.03\mathrm{fm}, 1.20\mathrm{fm}, 1.38\mathrm{fm})$

Summary

Provisos

- use of preliminary lattice scale and renormalization factors for exploratory study

Conclusions

- set up for baryonic observables on open bcs

Next

- O(a) improvement
- increased number of measurements, possibly add one source-sink separation to better constrain summation method analysis
- use all available ensembles to control chiral and continuum behaviour
- G_A, G_P, g_T, g_S, ...
- renormalization with RI'-(s)MOM on periodic bcs with Regensburg